ACS APPLIED MATERIALS & INTERFACES

Research Article

www.acsami.org

Mechanics of Platelet-Reinforced Composites Assembled Using Mechanical and Magnetic Stimuli

Rafael Libanori,[†] Randall M. Erb,[‡] and André R. Studart*[,†]

[†]Complex Materials, Department of Materials, ETH Zurich, 8093 Zurich, Switzerland

[‡]Department of Mechanical and Industrial Engineering, Northeastern University, Boston, Massachusetts 02115, United States

Supporting Information

ABSTRACT: Current fabrication technologies of structural composites based on the infiltration of fiber weaves with a polymeric resin offer good control over the orientation of long reinforcing fibers but remain too cumbersome and slow to enable cost-effective manufacturing. The development of processing routes that allow for fine control of the reinforcement orientation and that are also compatible with fast polymer processing technologies remains a major challenge. In this paper, we show that bulk platelet-reinforced composites with tailored reinforcement architectures and mechanical properties can be fabricated through the directed-assembly of inorganic platelets using combined magnetic and mechanical stimuli. The mechanical performance and fracture behavior of the resulting composites under compression and bending can be deliberately tuned by assembling the platelets into designed microstructures. By combining high alignment degree and volume fractions of reinforcement up to 27 vol %, we fabricated platelet-reinforced composites that can potentially be made with cost-effective polymer processing routes while still exhibiting properties that are comparable to those of state-of-the-art glass-fiber composites.

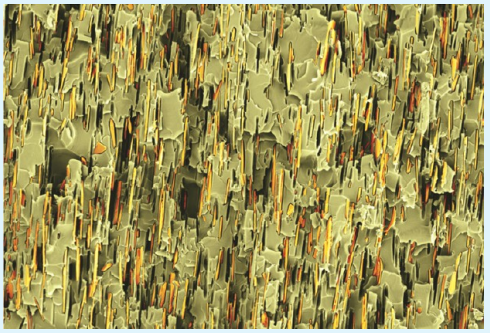

KEYWORDS: *bioinspired composites, platelet-reinforced composites, magnetic alignment, hybrid materials, tailored microstructures, micrometer-sized platelets*

INTRODUCTION

Composite materials have been increasingly used in load-bearing mobile applications mainly because of their high strength-to-weight ratio compared with that of their metallic counterparts. Despite their growing importance as a structural material, the cost of conventional long-fiber composites remains prohibitive in many applications partly because of both the inability of current manufacturing technologies to produce components with high volume fractions of fillers at rapid rates and also the incorporation of costly steps, such as impregnation of the fiber mat with polymeric resins and curing under autoclave conditions. In contrast, processing of composites reinforced with discontinuous fibers and platelets is simpler and more cost-effective, relying on conventional methods used in the bulk production of polymeric materials such as mold casting, injection molding, and extrusion. Further, these production techniques can lead to composite materials with far more intricate geometries than their continuous fiber counterparts. However, to take full advantage of the reinforcing effect of fibers and platelets in discontinuous particle-reinforced composites one needs to align them in specific directions or within a given plane of the composite.[1] Although flow-based processing techniques have been developed to partially address this requirement,[2−5] unusual geometries create distorted shear fields that destroy the ability to orient and distribute the reinforcing elements throughout the polymeric matrix. Therefore, devising approaches to control the orientation of reinforcing particles in any deliberate direction independently from the shear history of the fluid would enable new reinforcement design strategies for the production of durable and cost-effective composites in several applications in the automobile, aerospace, construction, and biomedical industries.

While deliberate control over the orientation of reinforcing particles has long been a challenge in synthetic composites, biological composites like mollusk shells,[6] bone,[7,8] and teeth[9] provide unique natural examples of accurate spatial and orientational distribution of reinforcing elements at multiple length scales.[10,11] Inspired by such biological architectures, several synthetic routes have been proposed to obtain well-ordered microstructures in platelet-reinforced composites, including tape-casting,[12] layer-by-layer,[13] electrical fields,[14] and gel casting combined with hot-pressing.[15,16] These approaches usually yield composites exhibiting superior in-plane mechanical properties, but are often limited to thin films and/or require multiple processing steps.[17] Bulk composites displaying a fairly high degree of platelet alignment or unique lamellar structures have also been obtained by hot-press assisted slip casting,[18] flow-induced alignment of fibers followed by filtration and polymer impregnation,[19,20] and freeze-casting of particle suspensions followed by sintering and polymer

Received: July 23, 2013
Accepted: October 8, 2013
Published: October 8, 2013

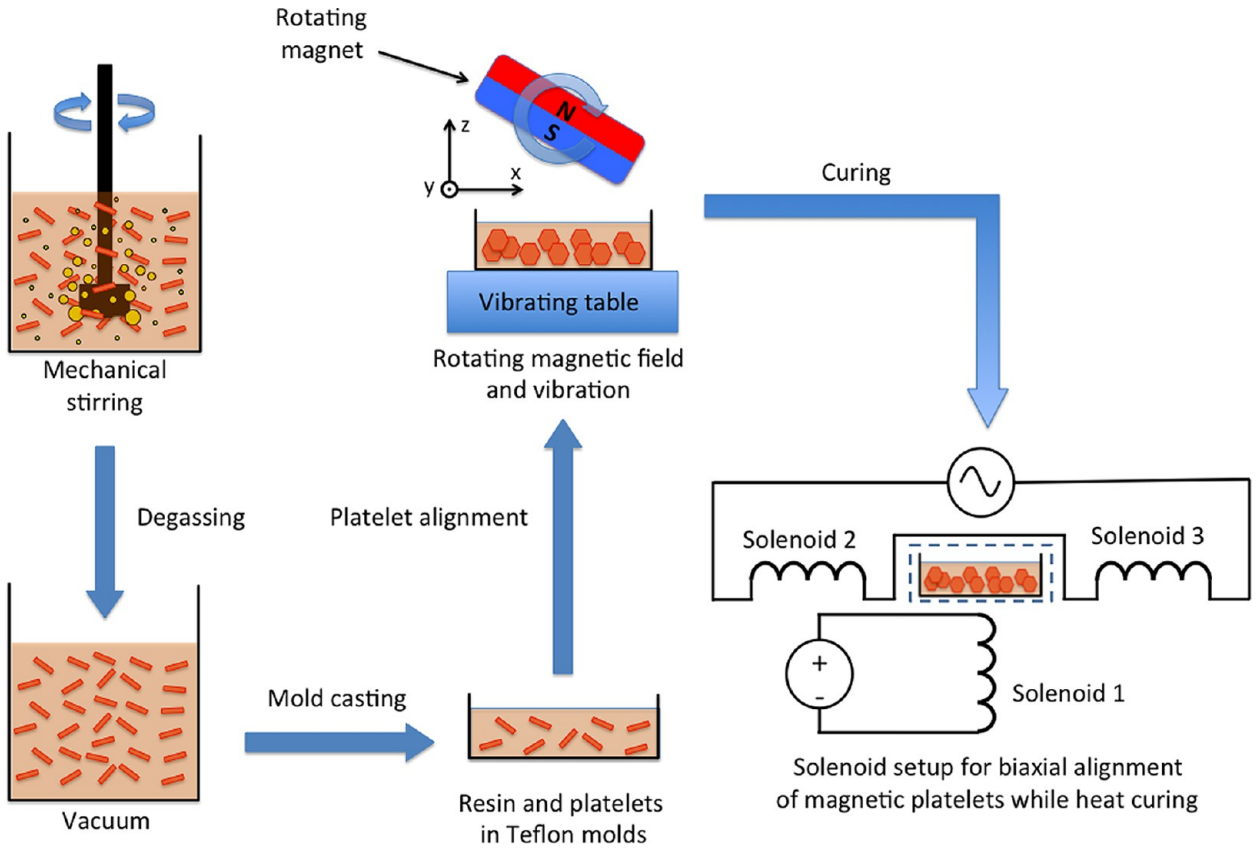

Figure 1. Processing route for the production of platelet-reinforced composites with tailored architectures using mechanical and magnetic stimuli. Solenoids are used to keep the alignment of the UHMR-platelets while curing the composites inside an oven at 60 °C.

infiltration.[21] Although lamellar materials with remarkable mechanical properties have been obtained, these approaches cannot be easily implemented in current polymer processing technologies to enable the envisioned low-cost fabrication of composites reinforced with short fibers and platelets.

Conversely, the directed-assembly of anisotropic particles in polymer melts or in monomer mixtures may be an effective means to deliberately control the reinforcement architecture of composites using conventional polymer processing methods. Recently, we proposed a strategy to align anisotropic non-magnetic platelets and rods in specific orientations using very low external magnetic fields.[22] The approach relies on coating reinforcing microparticles with superparamagnetic iron oxide nanoparticles (SPIONs) to remotely control their orientation and position within a fluid using standard, external magnets. Remarkably, SPION-coated microplatelets were found to exhibit ultrahigh magnetic response (UHMR), enabling control over their alignment using magnetic fields as low as 0.8 milliTesla in low-viscosity suspending fluids. Such fluids can be then consolidated to fix the magnetically-imposed alignment and thus create composites with tailored reinforcement architectures. Although magnetic assembly of anisotropic reinforcing particles has already been demonstrated in polymer nanocomposites, it often requires either the use of ferromagnetic reinforcing particles[23] or high magnetic fields (typically >1 Tesla).[24] Our earlier investigations have also shown that the magnetic alignment of alumina platelets in the direction of externally applied mechanical load is an effective strategy to improve the mechanical properties of polymer-based composites.[22] Because of the remarkable increase in the viscosity of fluids containing platelet concentrations above a percolation threshold, the major challenge in this approach is to obtain a high degree of alignment in composites loaded with high volume fractions of reinforcing particles. A deeper understanding of the structure-property relationships of such magnetically structured composites should allow us to quantify and predict the level of reinforcement achievable in these composite architectures.

In this paper, we thoroughly investigate the mechanical properties of platelet-reinforced epoxy-based composites exhibiting well-controlled reinforcement architectures obtained by the directed-assembly of UHMR alumina platelets using mechanical vibration and magnetic fields. The mechanical properties of as-cast and aligned composites are compared and explained in light of their underlying microstructures. We show how the simultaneous use of mechanical and magnetic stimuli can be effective in obtaining composites with high degree of platelet orientation and improved mechanical performance.

EXPERIMENTAL PROCEDURES

Materials. The epoxy system used throughout this work was kindly supplied by Huntsman Co, U.S.A. It is composed of a bisphenol A-based resin (Araldite GY250), an anhydride-based hardener (Aradur 917), and a tertiary amine-based catalyst (Accelerator DY070). Micrometer-sized alumina platelets (AlPearl) were provided by Antaria, Australia. Size analysis using scanning electron microscope (SEM) images revealed that the platelets exhibit average diameter of 12.66 ± 2.28 μm and average thickness of 0.36 ± 0.08 μm, leading to an average aspect ratio of 35.2 (Figure S1 in the Supporting Information). The aqueous-based anionic ferrofluid (EMG 705) used to magnetize the alumina platelets was purchased from Ferrotec Co., U.S.A. The ferrofluid contained 3.9 vol % SPIONs of nominal particle size of 12 nm suspended in water.

Magnetization of Alumina Platelets. Alumina platelets were magnetized by the electrostatic adsorption of SPIONs in deionized water. In a typical procedure, 0.375 mL of ferrofluid EMG 705 were diluted in 200 mL of water, and the resulting dispersion was added slowly to a suspension of 10 g of alumina platelets in 300 mL of water. Adsorption was carried out at room temperature and under magnetic stirring until the supernatant was clear. Magnetized platelets were removed from the suspension by vacuum filtration and washed with 1.5 L of water before a rinsing step with 200 mL of ethanol. Finally, the platelets were dried in an oven at 70 °C for 2 h. SEM images showing the distribution of SPIONs on the surface of the alumina platelets are depicted in Figure S2, Supporting Information.

Preparation of Platelet-Reinforced Composites. Figure 1 depicts the processing route used to prepare composites with deliberate reinforcement architectures using mechanical and magnetic stimuli. Prior to the preparation of the composites, magnetized platelets were dried in a vacuum oven under 30 mbar at 150 °C for 12 h. Next, the total amount of dried platelets was divided into three portions that were added sequentially in three separate steps into the stoichiometric mixture of Araldite GY250 resin and Aradur 917 hardener. For each addition, the resulting mixture was mechanically stirred with a mechanical mixer for 30 minutes at a speed of 2000 rpm. The bubbles introduced during the mixing step were removed by applying alternating cycles of vacuum (10 mbar; 60 °C) and ultrasonication (degassing mode, 45 kHz, 100 W). The degassing procedure was typically applied during 2−4 h, depending on the platelet concentration in the final composite mixture. After the addition of all the platelets, the catalyst was added into the degassed mixture and mixed carefully with a spatula to prevent the incorporation of additional bubbles. Finally, the mixture was degassed again and poured into a Teflon mold with dimensions of 3.5 cm × 4.5 cm × 1.0 cm.

Directed-Assembly of Platelets and Curing of the Composites. The Teflon mold containing the composite mixture was placed onto a vibrating table (Fritsch, type 03 502) and positioned under a 5.0 cm × 5.0 cm × 2.0 cm rare earth magnet (Supermagnete, Switzerland), connected to a small motor (Figure 1). The permanent magnet was rotated at a frequency of 4 Hz to produce a rotating magnetic field of about 1040 G in the $x-z$ plane of the coordinate system shown in Figure 1. Concurrently, continuous mechanical vibration was applied to the sample at the maximum power of the vibrating table (500 W) for 10 minutes. Platelet alignment takes place during the first 2 minutes and can be observed by changes of the surface color of the resin. Afterwards, the epoxy composite was kept under the rotating field for 12 h to increase the viscosity of the polymer resin and avoid sedimentation of the platelets during subsequent curing in the oven. The sample was then transferred to an oven held at 60 °C and exposed to an additional oscillating magnetic field of about 250 G for 4 h. The oscillating field was composed of the superposition of a static magnetic field in the z-axis and an alternating magnetic field along the x-axis. The magnetic fields were generated by three computer-programmed solenoids, as depicted in Figure 1. The oscillating field was produced by two solenoids connected in series and positioned horizontally on either side of the sample, while the vertical field was produced by a third solenoid positioned vertically below the specimen. The current passing through the solenoids was provided by two Bipolar Operational Power Supplies (20-5M, Kepco, U.S.A.) and controlled via a A/D board (CYDAS 1602HDP, CyberResearch, U.S.A.) using a LabView program. A sinusoidal waveform with frequency of 3 Hz was set to control the amplitude of the current in the horizontal solenoids whereas a static current was driven to the vertical solenoid. Afterwards, the sample was removed from the magnetic field setup and subjected to a final heat treatment of 4 h at 100 °C. In this study, composites designated "as-cast" were subjected only to mechanical vibration during casting but not to the magnetic fields.

Characterization. The microstructures of the platelet-reinforced composites were assessed by imaging polished or freshly fractured surfaces of the specimens under a scanning electron microscope (SEM, LEO 1530, Zeiss). To obtain smooth surfaces, samples were cold embedded into low viscosity epoxy resin, ground with silicon carbide foils (grits: 600, 1200, 2400, and 4000) and finally polished with diamond suspension (grain size: 3 μm and 1 μm) and colloidal alumina suspension (particle size: 50 nm). Fractured surfaces were obtained from samples cleaved during the flexural tests.

The alignment of alumina platelets within the x-axis (Figure 1) was measured by X-ray diffraction (XRD) using the rocking curve technique.[25] In this method, a high-resolution scan along the x-axis of the sample is first acquired at high 2θ angles ($88° > 2\theta > 92°$) and the most intense diffraction peak is selected. The 2θ angle corresponding to the 0012 crystallographic plane ($2\theta = 90.7°$) is then fixed, and the sample is slowly rocked by an angle ω while acquiring the data. The data is then corrected for tilt-defocusing and absorption effects using the software TexturePlus, which was kindly supplied by Dr. Mark Vaudin (NIST, Gaithersburg, MD, U.S.A.). All XRD measurements were performed in an Empyrean diffractometer (PANalytical).

Compression tests were performed on cylindrical samples with a diameter of 5 mm and a height of 10 mm using a Zwick universal mechanical testing machine (model Z250) at a displacement rate of 1 mm/min. Flexural tests were carried out on bars measuring 3 mm × 5 mm × 4.5 mm, which were machined from larger blocks and ground with 600, 1200, 2400, and 4000 grit SiC paper. An Instron 4411 universal mechanical testing machine equipped with a three-point bending rig was used for the bending tests. Bending was applied using a load line displacement rate of 5 mm/min with a span of 30 mm between the static supports. Load−displacement curves were corrected for machine compliance. At least three samples were measured to obtain the reported average and standard deviation values.

A Wolpert Microhardness Tester (MXT-α) was used to measure Vickers hardness. Samples were cold embedded in epoxy resin and polished according to the procedure described above. A thin layer of platinum (20 nm) was sputtered on the surface of the samples to increase light reflectivity and improve the accuracy of the measurement. For each sample, five measurements were carried out using a pyramidal indenter pushed into the sample surface with a force of 0.05 kgf for 15 seconds. Vickers hardness was calculated based on the arithmetic average length of the indent diagonals.[26]

The composite's resistance against crack initiation (K_{IC}) was measured on an Instron 8562 universal mechanical testing machine equipped with a strain gage to accurately measure the deflection of single-edge notched beams during mechanical loading. A span of 20 mm was used to test all samples. The thickness of the samples varied within the range 2.5−3.0 mm, and the width was accurately adjusted to obtain a span-to-width ratio of 4. Notches were prepared by first cutting the sample in a wire saw machine with wire diameter of 0.3 mm (Well model 3242) followed by continuously sliding a fresh razor blade with a custom-built machine. Calculations of the fracture toughness values were performed according to the ASTM standard D5045-99,[27] and the reported values are the average of at least 3 samples.

RESULTS AND DISCUSSION

Directed-Assembly of Micrometer-Sized Platelets. The ability to direct the assembly of UHMR alumina platelets into long-range well-ordered structures using magnetic fields is influenced by the volume fraction of platelets suspended in the precursor solution. UHMR alumina platelets with aspect ratio around 35 can be easily manipulated with external magnetic fields if their volume fraction is lower than approximately 10 vol %. For this reason, magnetically-structured advanced composites have been often processed using diluting solvents that reduce the concentration of platelets in the suspension.[22] Alignment of high volume fractions of platelets in the solvent-free systems utilized in polymer processing technologies is hindered by steric interactions between the microparticles, which prevent the system from reaching its most thermodynamically stable configuration of complete alignment.

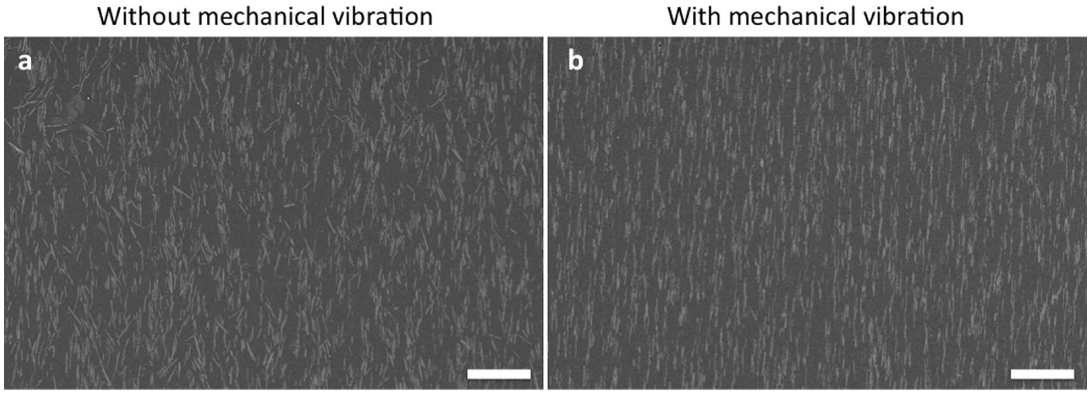

Figure 2. SEM images of polished surfaces showing the microstructures of (a) non-vibrated and (b) vibrated composites with biaxially-aligned UHMR-alumina platelets. The volume fraction of platelets is 11%. Scale bars: 40 μm.

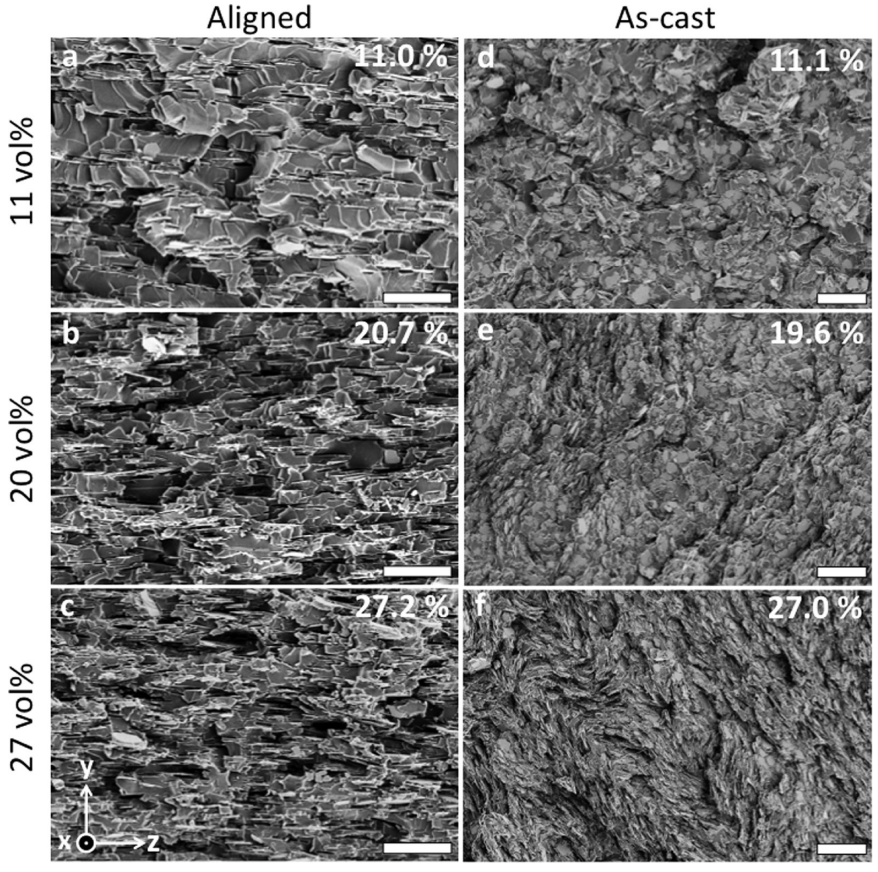

Figure 3. SEM images showing the fractured surfaces of (a–c) aligned and (d–f) as-cast samples at different volume fractions. Scale bars are (a–c) 20 μm and (d–f) 40 μm.

We found that the application of mechanical vibration during the magnetic alignment process provides enough kinetic energy to the platelets to favor their rearrangement and alignment along the plane of the rotating magnetic field. Figure 2 depicts the effect of mechanical vibration on the microstructure of a composite containing 11 vol % of UHMR platelets. When a rotating magnetic field is applied alone (Figure 2a), steric hindrance between neighbor platelets limits their movement and thus impedes full alignment of their long axis along the plane of the applied rotating magnetic field. Remarkably, the simultaneous use of mechanical vibration and magnetic fields leads to microstructures exhibiting a much higher degree of alignment, as shown in Figure 2b. The effect becomes more significant as the volume fraction of the platelets is increased, since steric hindrance plays a stronger role in restricting platelet movement in the suspension.

By applying simultaneously mechanical and magnetic stimuli, we are able to assemble these platelets into highly ordered structures with platelet volume fractions up to 27% (Figure 3a–c). To achieve biaxial alignment of platelets suspended in a liquid of viscosity η, the frequency ω of the external rotating magnetic field must be higher than a critical frequency ω_c, defined as[28]

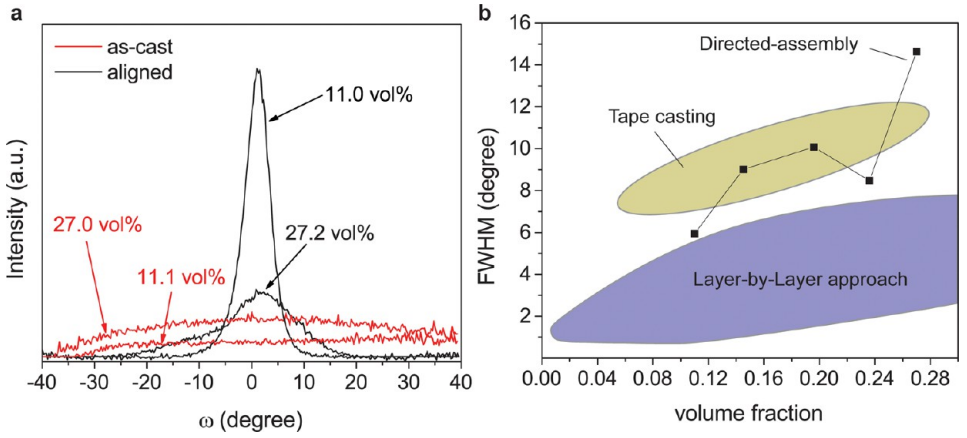

Figure 4. (a) Corrected rocking curves comparing the long-range structural order of samples prepared with magnetic and mechanical stimuli (black lines) and only mechanical vibration (red lines). (b) Full width at half maximum (FWHM) of the angular distribution curve as a function of the volume fraction of platelets in samples exhibiting long-range structural order (aligned). The bluish and yellowish regions show the FWHM values previously obtained for platelet-reinforced composites produced by tape-casting and a layer-by-layer approach.[13,37]

$$\omega_c = \frac{\mu_0 \chi_{ps}^2 H_0^2}{18(f/f_0)\eta(\chi_{ps}+1)} \cdot \left[\frac{(a+d)(b+d)^2}{ab^2} - 1\right] \quad (1)$$

where H_0 is the intensity of the magnetic field; a and b are half the average thickness and half the average diameter of the platelets, respectively; d is the diameter of the SPION; μ_0 is the magnetic permeability of free space; χ_{ps} is the magnetic susceptibility of the platelet shell and f/f_0 is the Perrin friction factor.[29] The magnetic susceptibility χ_{ps} can be estimated from the packing fraction of SPIONs in the platelet shell. For a magnetic field strength of 1040 G and magnetic susceptibility χ_{ps} of 3.47, the critical frequency for biaxial alignment of platelets in a fluid with viscosity of 900 mPa s is approximately 0.5 Hz. A surface coverage of SPIONs on the platelet surface φ_{np} of 0.165 and a magnetic susceptibility of SPIONs χ_{SPION} of 21 were assumed in these calculations.[30] To ensure biaxial alignment of the UHMR platelets within the $x-z$ plane, the north-south magnetic axis of a rare-earth magnet is rotated at a frequency higher than the critical value of 0.5 Hz (eq 1) within the $x-z$ plane of the coordinate system shown in Figures 1 and 3. At such high frequency, the platelets align their long axis along the plane of the applied rotating field as the viscous drag forces exerted on the platelets become too high to allow them to roll with the rotating magnetic field.[28,31]

To better understand the effect of magnetic fields on the alignment of UHMR platelets at high volume fractions, we also investigated the reinforcement orientation obtained under mechanical vibration alone. In the absence of magnetic fields, packing entropic effects are expected to induce ordering of the platelets into nematic-like domains.[32−35] The assembly of particles into nematic-like domains occurs when the volume fraction of platelets (ϕ_p) surpasses the critical concentration expected for the isotropic-nematic (I−N) phase transition. For platelets exhibiting an aspect ratio of 35.2 and a polydispersity of 0.18, we expect that a nematic phase co-exists with an isotropic phase for $9.9 < \phi_p < 11.9$ vol % and eventually becomes the stable phase at $\phi_p > 11.9$ vol % (see Supporting Information for further details).[32,36] In agreement with such predictions, nematic-like domains exhibiting platelets oriented in the same direction can be identified in the non-vibrated and vibrated composites (Figure 3e,f and Figure S3 in the Supporting Information). Interestingly, such nematic-like domains grow when suspensions are subjected to mechanical vibration (see Figure S3 in the Supporting Information). This indicates that the supply of additional energy into the suspension provides enough kinetic energy to the platelets to explore other configurations and eventually re-arrange themselves into larger domains that increase the overall entropy of the system. Despite such local ordering of platelets within each nematic-like domain, the structure does not show long-range ordering as the domains with different platelet orientations are randomly distributed throughout the matrix.

The long-range ordering and the degree of platelet alignment within the x-axis of the composites were experimentally assessed through an X-ray diffraction technique called rocking curve or omega-scan (see Experimental Procedures).[25] The results revealed no defined diffraction peak in the omega-scan for the as-cast specimens, suggesting that no long-range preferential alignment of the platelets exists in samples that were not exposed to magnetic fields (Figure 4a, red lines). Instead, samples subjected to mechanical vibration and rotating magnetic fields (Figure 4a, black lines) exhibit a well-defined peak at an omega angle of about 0°, indicating preferential alignment of the platelets within the x-axis of the composite. The degree of misalignment of the anisotropic platelets was semi-quantitatively described by the full width at half maximum (FWHM) of the obtained angular distribution, which is shown as a function of the volume fraction in Figure 4b. Samples with volume fractions lower than 25 vol % exhibit reasonably high degree of platelet alignment within the x-axis, as revealed by the FWHM values below 10.1°. However, stronger misalignment (FWHM = 14.65°) is observed for the sample containing 27.2 vol % of alumina platelets. This is probably caused by the strong steric interactions between platelets and the very high viscosity of the platelet-epoxy resin mixtures at such high concentrations of inorganic particles, which eventually jam the system and impede it from achieving the thermodynamically favorable aligned configuration.

Surprisingly, the degree of alignment achieved for composites processed through the directed-assembly route is not so far from that typically obtained by the laborious and cumbersome layer-by-layer approach[13,37] (bluish regions in Figure 4b) and is even comparable to that observed in composite films produced by tape casting (yellowish region in Figure 4b).[12] In addition to such high control over platelet alignment, the method outlined

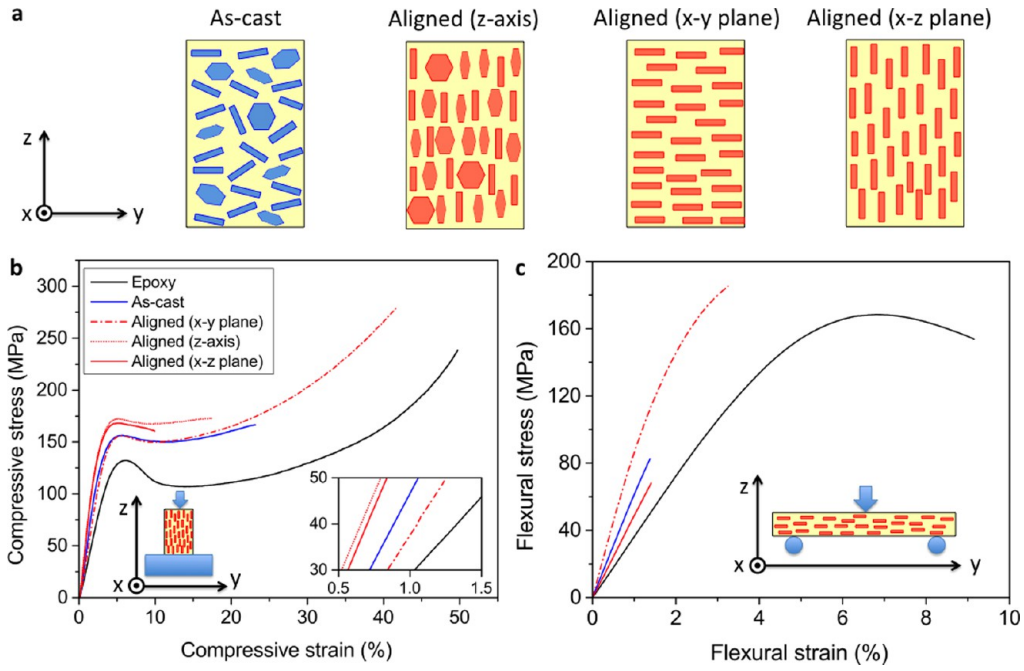

Figure 5. (a) Schematics of the investigated model composite architectures. Blue and red colors represent bare and magnetized platelets, respectively. (b,c) Effect of the microstructure on the mechanical response of composites containing 11.5 vol % of platelets subjected to (b) compression and (c) bending.

here allows for the fabrication of bulk samples with platelets oriented in any deliberately chosen direction. Moreover, its directed-assembly nature makes this route compatible with technologies currently used in the production of polymers and composites.

Structure-Property Relationships in Tailored Reinforcement Architectures. Control over the orientation of reinforcing platelets is crucial for tailoring the mechanical response of the composites. To investigate the correlation between reinforcement architecture and the mechanical properties of the epoxy-based composites, we designed and assembled the series of model microstructures schematically shown in Figure 5a. In addition to the as-cast samples, three different aligned architectures containing 11.5 vol % of platelets were created. In one of the aligned configurations, platelets were oriented uniaxially along the z direction using a static magnetic field. In this case, platelets are free to rotate around their long axis. This increases disorder and steric interactions between neighbor particles, limiting the platelet volume fraction in the system. The other two aligned configurations were obtained using a rotating magnetic field that enables biaxial orientation of the platelets within a specific plane of the composite, namely, the x−y or the x−z planes. Such model composites were mechanically tested under compression and bending.

Representative stress-strain curves obtained for composites tested under compression are depicted in Figure 5b. Composite architectures with platelets aligned uniaxially (z-axis) or biaxially (x−z plane) along the loading direction exhibited the highest averaged increase in compressive elastic modulus (E) and yield strength (σ_y). The E and σ_y values for such composites were approximately 120% and 30% higher than those for the neat epoxy, respectively. While no significant difference in compressive elastic modulus and yield strength was observed between samples reinforced in the loading direction, biaxially oriented platelets (x−z plane) were found to reduce significantly the overall strain at rupture as compared with uniaxially aligned particles (z axis). The 35% lower strain at rupture results from the preferential reinforcement of only one of the planes parallel to the loading direction (x−z plane). This stronger reinforcement in one specific plane leads to premature failure of the material at lower compressive strains because the expected deformation of the polymer matrix in the radial direction is significantly constrained within that reinforced plane, limiting ultimately the compressive strain at rupture of the whole composite. Conversely, composites biaxially reinforced perpendicular to the loading axis (x−y plane) allow for a much larger shear deformation of the matrix in the radial direction. As a result, these composites exhibit strain at rupture nearly as high as those achieved with the neat epoxy (44.5%), despite reaching E and σ_y values comparable to those of the as-cast specimens. As-cast composites were significantly stronger and stiffer than neat epoxy, showing a relative increase in compressive elastic modulus and yield strength of 79% and 55%, respectively, as compared to the pure polymer. Additional experiments showed that the presence of magnetic nanoparticles on the alumina surface does not affect the mechanical properties of as-cast composites (See Figure S4 in the Supporting Information).

The effect of platelet alignment on the bending properties of epoxy-based composites was also investigated, as shown in Figure 5c. Strong reinforcement and clear inelastic deformation is observed for composites containing platelets oriented longitudinally with respect to the long-axis of the bending sample (x−y plane). In such configuration, the plane containing aligned platelets coincides with the plane of the sample where the highest normal stresses are expected. For the 3-point bending configuration used in these experiments, the maximum normal tensile stresses occur within the x−y plane under the loading line at the bottom of the sample. At the microscale, reinforcement takes place through the development of shear forces at the platelet-matrix interface, which ultimately lead to

stress transfer from the softer polymer matrix to the stiffer and stronger inorganic platelets. As a result of such reinforcing effect, samples with longitudinally aligned platelets ($x-y$ plane) exhibited an average increase in flexural modulus and maximum strength of 124% and 10% as compared to the pure polymeric matrix, respectively. These values are at least 2.5-fold higher than those shown by as-cast composites. The major increase in elastic modulus clearly reflects the reinforcing effect of the aligned alumina platelets. This reinforcing effect is less evident in the strength data, most likely because of the high stress concentration in the confined polymer matrix, which results in cracking of the polymer before significant stress can be transferred to the stiff platelets. In contrast to such reinforcing effect, composites with random microstructure (as-cast) or containing platelets aligned transversely ($x-z$ plane) exhibit brittle failure and rupture at much lower stresses than even the neat epoxy polymer (Figure 5c). These results indicate that the presence of platelets aligned perpendicular to the plane of maximum tensile stresses significantly degrades the mechanical properties of polymer matrices exhibiting limited ductility as the epoxy studied in this work. Although this degrading effect is stronger in the fully aligned sample ($x-z$ plane), the very low strength of the as-cast composites suggests that the presence of only a fraction of transversely oriented platelets in a random microstructure is already enough to significantly reduce the ultimate strength of the composite. Local stress concentration at the boundaries between adjacent nematic-like domains with different internal platelet orientations might further contribute to this degrading effect in as-cast composites.

Overall, these results show a strong effect of the microstructure on the mechanical behavior of the composite. This makes it possible to achieve the mechanical response required in specific applications, by simply tuning the microstructure of the composite without changing the concentration of reinforcing particles and the overall chemistry of the material. Under compressive loads, applications requiring the highest compressive stiffness and strength but with minimum reduction in strain at rupture would be best served if the composite contains platelets uniaxially aligned in the compressive loading direction (z-axis aligned in Figure 5a). In contrast, situations requiring the highest strain-at-rupture but yet significant reinforcement would make the composites biaxially reinforced in the $x-y$ plane a better choice. Under bending, the best performing microstructure is the one exhibiting platelets aligned in the plane where the normal stresses are developed during loading ($x-y$ plane). This configuration leads to enhanced flexural modulus, maximum flexural strength and strain at rupture. Microstructures containing random or fully aligned platelets in the $x-z$ plane improve the flexural modulus but seriously degrade the maximum flexural strength and strain at rupture. This comparative analysis is valid for composites containing low concentrations of platelets (11.5 vol %). Because the processability and resulting degree of alignment within the composites are affected by the volume fraction of platelets (Figure 4), different trends may prevail for materials obtained with higher concentrations of reinforcing particles. To understand how the volume fraction of platelets may change this comparative analysis, the effect of platelet concentration on the mechanical response of such composites in specific loading conditions is investigated below.

Flexural Properties. In addition to the effect of platelet orientation, we also investigated the flexural properties of as-cast and aligned composites ($x-y$ plane) with increasing volume fractions of reinforcement. As depicted in Figure 6a, both as-cast and aligned composites showed improved flexural

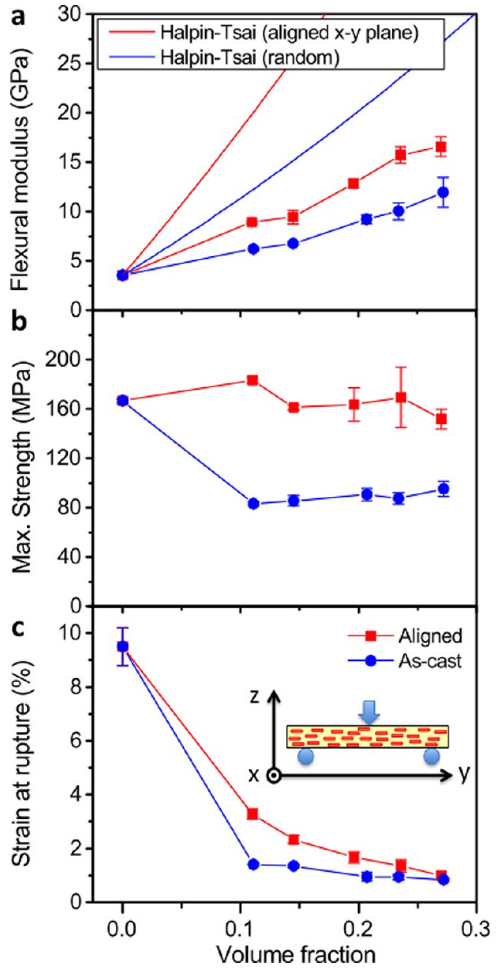

Figure 6. Effect of the volume fraction of platelets on the (a) flexural elastic modulus, (b) flexural strength, and (c) strain at rupture of as-cast and aligned composites.

modulus (E) for increasing volume fractions of platelets. In agreement with the results presented above, composites containing platelets aligned in the $x-y$ plane exhibited higher E values. Remarkably, flexural modulus as high as 16.6 GPa is obtained in the aligned composite with 27.2 vol % of platelets, which is 1.4-fold and 4.7-fold higher than those exhibited by the equivalent as-cast and pure polymeric matrix, respectively. Such flexural modulus is comparable to the level obtained using conventional long-fiber composites, which typically require longer processing cycles (as discussed later). The E values at different volume fractions were compared to predictions of the Halpin–Tsai model, which provides quantitative estimates of the elastic modulus of composites displaying random and aligned platelet architectures.[38,39] Despite the reinforcing effect observed for both composites, their elastic moduli are far below the values predicted by the Halpin–Tsai model. This difference may arise from the deviations of the idealized composite microstructure assumed in the theoretical model. For instance, the model assumes that the matrix and the reinforcing platelet are linearly elastic, isotropic, and perfectly bonded. The usual difficulties in achieving the theoretical perfect bonding in real systems might be one of the reasons for the observed

inconsistency between theory and experiments. Moreover, the platelets in the model are considered perfectly aligned with a uniform size distribution and shape, and the interactions between adjacent platelets at high volume fractions are neglected. All these idealized conditions, particularly the perfect alignment of platelets, are not representative of the actual microstructure of the investigated composites.

Although the bending stiffness of the aligned composites improved with increasing volume fractions of reinforcement, their maximum flexural strength values were only marginally affected by the concentration of platelets (Figure 6b). The values obtained for the aligned composites lie within ±10% of the value exhibited by the neat epoxy. The sub-optimal interfacial adhesion between the bare platelets and the matrix,[40] the incorporation of voids during composite fabrication,[16] and the low ductility of the polymer matrix might be the main causes for limiting the increase in maximum strength expected for the aligned composites. In fact, literature data show that significant strengthening of epoxy polymers using stiff particles is often a challenge. Several studies actually report unchanged or even lower strength values upon addition of discontinuous stiff reinforcements.[40−44] A deleterious effect on the composite strength was observed in the as-cast specimens, which showed maximum strength of approximately half of those of the pure epoxy matrix and of the aligned composites. These strength data for aligned and as-cast specimens are in good agreement with the results obtained for the series of composites with different architectures under three-point bending (Figure 5c). As discussed earlier, the low fraction of misaligned platelets and the random orientation of nematic-like domains in the as-cast specimen may be sufficient to significantly degrade the mechanical strength of the composite under bending. This strength-degrading effect may occur because of the high stresses that might develop at the boundary between adjacent nematic-like domains with different internal platelet orientations or at the sharp edge of platelets aligned in unfavorable directions. The resulting stress concentration at these sites is expected to be more pronounced in polymer matrixes of low ductility like the epoxy investigated here. The ultimate ductility of the composite is also impaired by the stress concentration around misaligned platelets and between nematic-like domains, as evidenced in Figure 6c by the lower strain at rupture of the as-cast specimens. A recent study has shown that the surface modification of alumina microplatelets might compensate for these stress-concentrating effects and eventually allow for a simultaneous increase of the stiffness and strength of similar composites.[18]

Hardness. Surface hardness of the as-cast and aligned composites was assessed by loading the samples with a pyramidal diamond indenter in different directions with respect to the reinforced plane. The results revealed that the surface hardness enhances with increasing volume fractions of platelets for both aligned and as-cast composites (Figure 7). Specimens containing platelets preferentially aligned in the loading direction exhibit surface hardness significantly higher than those of as-cast composites, especially at volume fractions higher than 20%. Conversely, aligned composites loaded perpendicular to the reinforced plane show surface hardness only slightly lower than those of as-cast composites. The lack of preferential alignment in as-cast composites results in values of surface hardness that do not strongly depend on the loading direction. The larger error bars exhibited by the as-cast composites probably derive from the fact that the size of the indented area (approximately 50 × 50 μm^2) is at a similar length scale as the individual medium-range nematic-like domains that develop in these specimens (Figure 3e,f and Figure S3d in the Supporting Information). This leads to a larger data spread, since individual indentations might probe one nematic-like domain alone, which can vary widely in orientation for the as-cast microstructures.

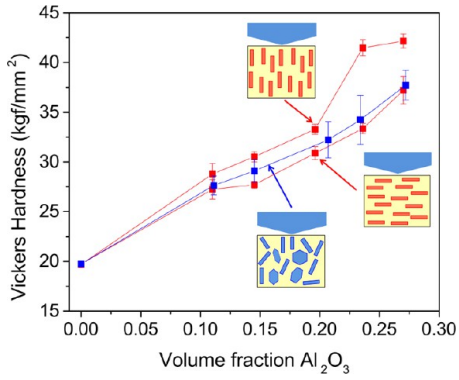

Figure 7. Vickers hardness as a function of the volume fraction of alumina platelets in as-cast specimens and aligned composites indented parallel and perpendicular to the platelet orientation.

Overall, our ability to control the microstructure of platelet-reinforced composites allows us to reach values of surface hardness that would not be possible to obtain otherwise for the same set of initial building blocks. The surface hardness of aligned composites loaded parallel to the platelet orientation reached a value as high as 42.2 kgf mm^{-2}, which is 115% and 11% higher than those of the pure matrix and the equivalent as-cast composite, respectively. Despite the complex multiaxial stress state developed under the indenter during the measurement, the alignment of platelets parallel to the loading direction is an effective approach to increase the composite's hardness.

Fracture Toughness. To further illustrate the benefit of controlling the microstructure of platelet-reinforced composites, we compared the resistance against crack initiation (K_{IC}) of a series of specimens exhibiting the as-cast and aligned platelet architectures (Figure 8). As opposed to the fracture strength (Figure 6b), the K_{IC} is an intrinsic property of the material that does not depend on processing surface flaws. Thus, the determination of the K_{IC} values of as-cast and aligned composites eliminates the possible masking effect of surface defects, allowing for a direct comparison of the different microstructures. To ensure strong stress concentration at the crack initiation site, notches with root radius of around 2−3 μm were prepared (Figure 8a) by first cutting one edge of the beam using a wire saw and then repeatedly sliding a fresh razor blade over the notch to sharpen the crack tip.

As with the orientation effect observed under bending mode (Figure 6b), composites containing platelets in the plane perpendicular to the crack propagation direction (x−y plane) result in better resistance against crack initiation as compared to conventional as-cast composites (Figure 8b). For platelet volume fractions between 10 and 25 vol %, the K_{IC} values of aligned samples were 24−56 % higher than those obtained for the as-cast composites. This clearly shows the property enhancement possible by controlling the composite microstructure. Composites containing 24 vol % of platelets aligned in the x−y plane presented fracture toughness of 2.56 MPa $m^{1/2}$, which is 4.7-fold higher than pure epoxy alone. The unexpected low value observed for the composite with 27 vol %

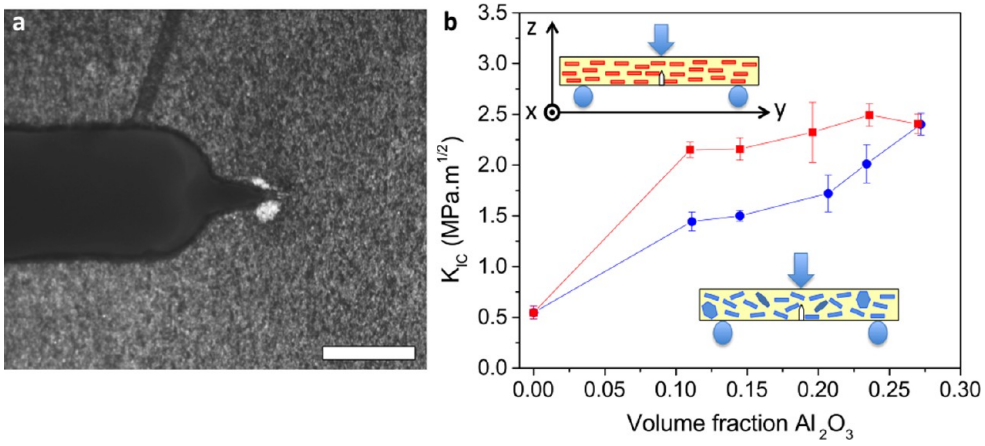

Figure 8. (a) Optical microscopy image of a typical sharp notch used to measure the resistance against crack initiation (K_{IC}) of the platelet-reinforced composites. Scale bar: 200 μm. (b) Dependence of the fracture toughness (K_{IC}) on the volume fraction of the platelets for as-cast and aligned composites.

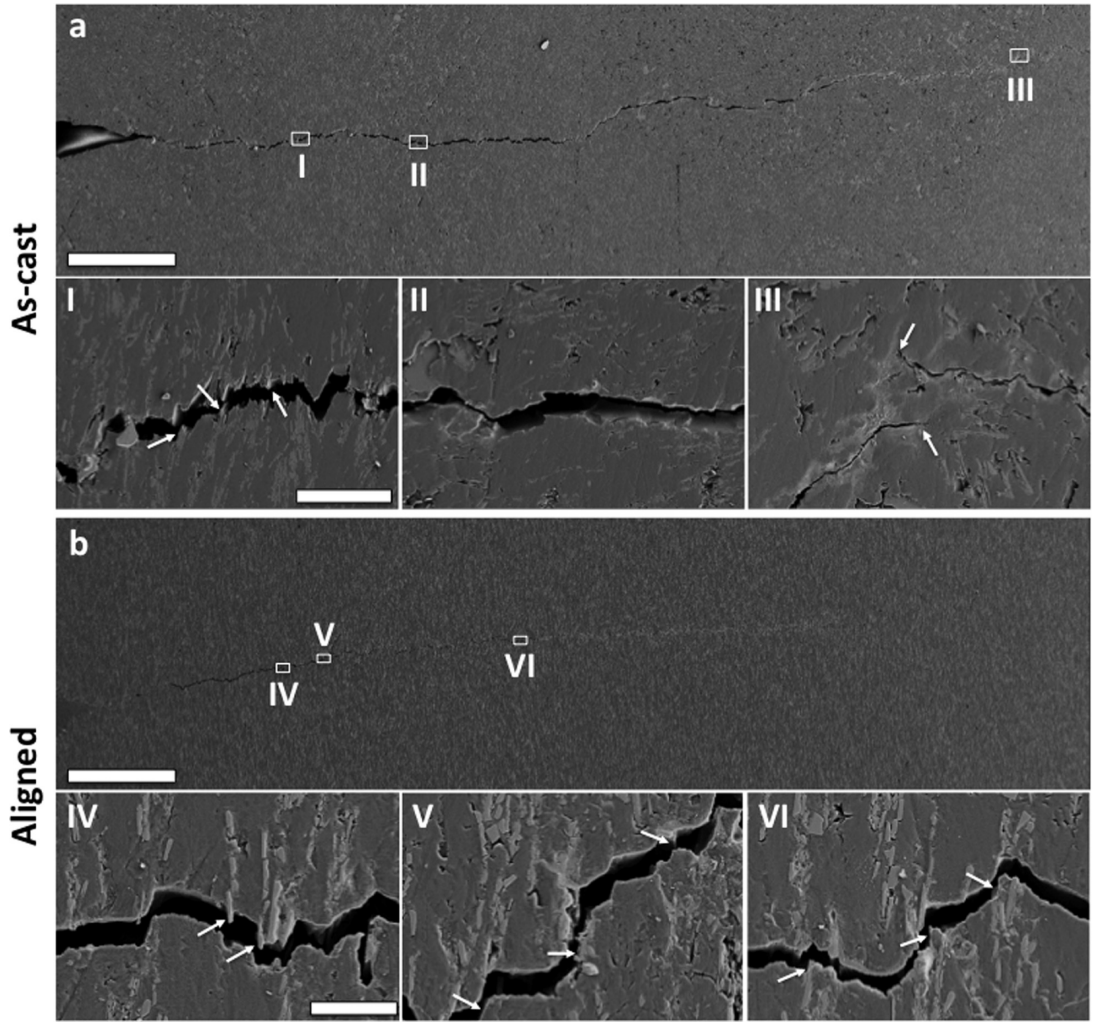

Figure 9. Visualization of the crack path in (a) as-cast and (b) long-range aligned composites after partial fracture of the notched specimens under bending. The regions I–VI depict some of the toughening mechanisms that take place during crack propagation. Scale bars: 200 μm in (a) and (b); 20 μm and 5 μm in the insets (a) and (b), respectively.

of aligned alumina platelets might be due to the high degree of platelet misalignment revealed by the texture measurements (Figure 4b). Surprisingly, the as-cast composite with 27 vol % of platelets showed a relatively high K_{IC} value of 2.37 MPa m$^{1/2}$, even though its mechanical performance under bending was significantly lower compared to the aligned composites. In general, the alignment of platelets in the direction of the highest tensile stresses enables an increase in the material's resistance

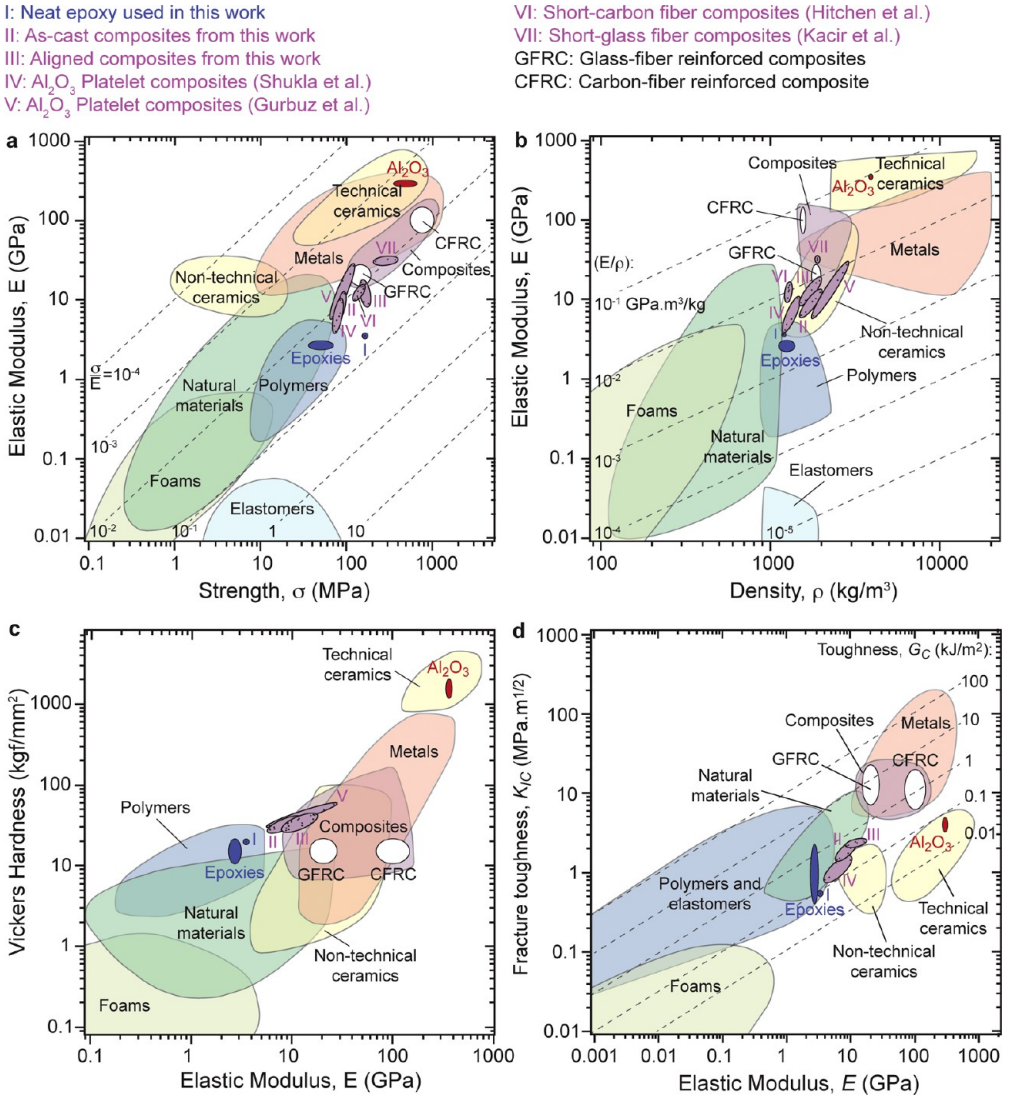

Figure 10. Ashby diagrams correlating the properties of the as-cast and aligned composites fabricated in this study with a wide range of materials and other similar composites published in the literature.[18−20,40] Diagrams (a), (b), and (d) were adapted with permission from Ashby.[45] Copyright 2005 Butterworth-Heinemann. Diagram (c) was adapted with permission from CES software, Granta Design Limited, Cambridge, UK, 2013 (www.grantadesign.com).[46]

against crack initiation at much lower reinforcement volume fractions than those required with conventional as-cast microstructures (Figure 8b).

In addition to enhancing the resistance against crack initiation, anisotropic reinforcing particles are expected to enable multiple toughening mechanisms during crack propagation throughout the composite. Indeed, ex-situ SEM images of partially fractured notched specimens containing 20 vol % of Al_2O_3 platelets suggest that several toughening mechanisms occur when the crack propagates through the microstructures with randomly oriented nematic-like domains and with long-range aligned platelets (as-cast and aligned specimens in Figures 9a,b).

We observe that the crack interacts differently with the microstructure depending on the local orientation of platelets. Platelets aligned perpendicular to the direction of crack propagation provide fracture resistance by multiple crack deflection events at the platelet-matrix interface (Region I, IV, V, and VI, Figure 9). In contrast, little interaction with the microstructure is found when the crack advances through nematic-like domains of the as-cast samples containing platelets aligned parallel to the propagation direction (Region II, Figure 9a). Despite the absence of crack deflection events, the lower elastic modulus of such parallel-aligned domains decreases the stress intensity factor at the crack tip enabling local arresting of the crack. We observe that such arresting effect at parallel-aligned domains occasionally induces crack initiation at another position of higher local elastic modulus and thus higher stress concentration within perpendicular-aligned domains (Region III). This leads to the formation of unbroken ligaments that increase the material's crack growth resistance through crack bridging (Region III). Other crack bridging and intrinsic toughening mechanisms are likely to occur but cannot be precisely identified in such ex-situ images because of the advanced stage of the fracture process. These results suggest that the composites presented in this study might exhibit crack growth resistance that increases with the crack length, namely, a rising R-curve behavior. Overall, the combination of crack deflection events within aligned nematic-like domains at the length scale of individual platelets (intra-domain toughening,

Region I) and crack bridging due to local differences in elastic modulus between domains at larger length scales (inter-domain toughening, Region III) indicate the rich set of multiscale toughening mechanisms that can occur in such platelet-reinforced composites.

Comparison with Other Short Fiber- and Platelet-Reinforced Composites. The mechanical performance of the composites reported in this study are compared in Figure 10 with data from a series of short fiber- and platelet-reinforced epoxy composites reported in the literature.[18−20,40]

Mechanical properties such as elastic modulus, fracture strength, and hardness were all found to lie in between the extreme values expected for pure epoxy and pure alumina. A more detailed analysis shows that even though the composites prepared in this study (Families II and III in Figure 10) contain relatively low volume fraction of reinforcing platelets (< 28%), their elastic modulus and strength may exhibit values that are comparable to those typically obtained for conventional composites reinforced with long glass fibers (GFRC, Figure 10a). This is a promising result, since it indicates that the directed-assembly route can potentially increase fabrication rates and cost-effectiveness while maintaining the same level of mechanical properties as those of current long-fiber composites.

The design lines shown in the elastic modulus *versus* density diagram (Figure 10b) also reveals that the directed-assembled composites perform particularly well in comparison with other materials if their weight-normalized specific elastic moduli are considered. This is especially important for the design of stiffness-driven structures with minimum weight. As far as surface hardness is concerned, we find that the presence of intrinsically stiffer and harder alumina platelets partially or fully aligned within the epoxy matrix results in composites with surface hardness significantly higher than those obtained with conventional long glass (GFRC) or carbon fiber-reinforced composites (CFRC) (Figure 10c).

Although the aligned composites described here exhibit crack-initiation fracture toughness lower than that of conventional GFRC and CFRC, the K_{IC} values achieved were found to be unusually high for their low reinforcement volume fraction and elastic modulus E (Figure 10d). This combination of high K_{IC} and low E leads to fracture energy levels G_C that surpass those observed for epoxy and pure alumina ($G_C = K_{IC}^2/E$). Design lines showing different G_C levels are included in Figure 10d to facilitate this comparison. In summary, this comparative study demonstrates the huge potential of tailoring the microstructure of platelet-reinforced composites to fulfill specific mechanical demands of targeted load-bearing applications.

CONCLUSIONS

The directed-assembly of reinforcing alumina platelets into ordered architectures using magnetic and mechanical stimuli leads to epoxy-based composites exhibiting tunable mechanical response. We show that the use of mechanical vibration during magnetic alignment is crucial to overcome steric hindrances between platelets and thus improve their degree of alignment, especially at higher volume fractions. The mechanical properties of the resulting composites under bending and compressive loads can be tuned following simple microstructural design rules without changing the concentration of reinforcing elements. In general, effective reinforcement against bending and compression is achieved by aligning the platelets in the direction where the highest normal tensile and compressive stresses are developed, respectively. Under the multiaxial stress state imposed by sharp indenters, we find that the alignment of platelets parallel to the loading direction is most efficient in increasing the surface hardness of the composite. With regards to the fracture process, our results suggest that several energy dissipation mechanisms take place during crack propagation throughout the platelet-reinforced microstructures. Composites created through the directed-assembly route exhibit mechanical performance comparable to those of long glass fiber-reinforced composites widely used as structural materials. Because of its easier scalability and compatibility with fast polymer processing technologies, the proposed directed-assembly approach should enable faster and more cost-effective processing of composite materials without compromising their unique mechanical properties.

ASSOCIATED CONTENT

Supporting Information

The supporting information contains the SEM image of SPIONs adsorbed onto alumina micro-platelets, analysis of the Ferret's diameter and thickness distribution of the micrometer-sized alumina platelets, effect of mechanical vibration on the microstructure of as-cast composites, and effect of magnetic functionalization on the compressive properties of platelet-reinforced composites. This material is available free of charge via the Internet at http://pubs.acs.org.

AUTHOR INFORMATION

Corresponding Author

*E-mail: andre.studart@mat.ethz.ch.

Notes

The authors declare no competing financial interest.

ACKNOWLEDGMENTS

We thank Prof. Jörg Löffler and Prof. Ludwig Gauckler for granting access to equipment from their laboratories, Dr. Kyrill Feldman, Nuria Rothfuchs, Davide Carnelli, Simon Bachmann, and Benjamin Hartmeier for their invaluable experimental support, Peter Kocher, Beatrice Wegmann, Martin Elsener, and Christian Roth for their technical assistance, Dr. Mark Vaudin for kindly providing the software TexturePlus, and Niklaus Kränzlin for his experimental assistance on XRD measurements.

REFERENCES

(1) Hull, D.; Clyne, T. W. *An Introduction to Composite Materials*; Cambridge University Press: Cambridge, U.K., 1996; p 326.
(2) Karmaker, A. C.; Youngquist, J. A. *J. Appl. Polym. Sci.* **1996**, *62*, 1147−1151.
(3) Kalaitzidou, K.; Fukushima, H.; Drzal, L. T. *Carbon* **2007**, *45*, 1446−1452.
(4) Huang, H.; Liu, C. H.; Wu, Y.; Fan, S. S. *Adv. Mater.* **2005**, *17*, 1652−1656.
(5) Fu, S. Y.; Lauke, B.; Mader, E.; Yue, C. Y.; Hu, X. *Composites, Part A* **2000**, *31*, 1117−1125.
(6) Jackson, A. P.; Vincent, J. F. V.; Turner, R. M. *Proc. R. Soc. London, Ser. B* **1988**, *234*, 415−440.
(7) Kerschnitzki, M.; Wagermaier, W.; Roschger, P.; Seto, J.; Shahar, R.; Duda, G. N.; Mundlos, S.; Fratzl, P. *J. Struct. Biol.* **2011**, *173*, 303−311.
(8) Koester, K. J.; Ager, J. W.; Ritchie, R. O. *Nat. Mater.* **2008**, *7*, 672−677.
(9) Maas, M. C.; Dumont, E. R. *Evol. Anthropol.* **1999**, *8*, 133−152.

(10) Dunlop, J. W. C.; Fratzl, P. *Annu. Rev. Mater. Res.* **2010**, *40*, 1−24.
(11) Fratzl, P.; Weinkamer, R. *Prog. Mater. Sci.* **2007**, *52*, 1263−1334.
(12) Libanori, R.; Münch, F. H. L.; Montenegro, D. M.; Studart, A. R. *Compos. Sci. Technol.* **2012**, *72*, 435−445.
(13) Bonderer, L. J.; Studart, A. R.; Gauckler, L. J. *Science* **2008**, *319*, 1069−1073.
(14) Lin, T. H.; Huang, W. H.; Jun, I. K.; Jiang, P. *J. Colloid Interface Sci.* **2010**, *344*, 272−278.
(15) Bonderer, L. J.; Feldman, K.; Gauckler, L. J. *Compos. Sci. Technol.* **2010**, *70*, 1966−1972.
(16) Bonderer, L. J.; Feldman, K.; Gauckler, L. J. *Compos. Sci. Technol.* **2010**, *70*, 1958−1965.
(17) Corni, I.; Harvey, T. J.; Wharton, J. A.; Stokes, K. R.; Walsh, F. C.; Wood, R. J. K. *Bioinspiration Biomimetics* **2012**, *7*, 031001.
(18) Gurbuz, S. N.; Dericioglu, A. F. *Mater. Sci. Eng., C* **2013**, *33*, 2011−9.
(19) Kacir, L.; Narkis, M.; Ishai, O. *Composites* **1978**, *9*, 89−92.
(20) Hitchen, S. A.; Ogin, S. L.; Smith, P. A. *Composites* **1995**, *26*, 303−308.
(21) Munch, E.; Launey, M. E.; Alsem, D. H.; Saiz, E.; Tomsia, A. P.; Ritchie, R. O. *Science* **2008**, *322*, 1516−1520.
(22) Erb, R. M.; Libanori, R.; Rothfuchs, N.; Studart, A. R. *Science* **2012**, *335*, 199−204.
(23) Hammond, M. R.; Dietsch, H.; Pravaz, O.; Schurtenberger, P. *Macromolecules* **2010**, *43*, 8340−8343.
(24) Koerner, H.; Hampton, E.; Dean, D.; Turgut, Z.; Drummy, L.; Mirau, P.; Vaia, R. *Chem. Mater.* **2005**, *17*, 1990−1996.
(25) Vaudin, M. D.; Rupich, M. W.; Jowett, M.; Riley, G. N.; Bingert, J. F. *J. Mater. Res.* **1998**, *13*, 2910−2919.
(26) ASTM E384-11 e1: Standard Test Method for Knoop and Vickers Hardness of Materials. 2012.
(27) ASTM D5045-99(2007)e1: Standard Test Methods for Plane-Strain Fracture Toughness and Strain Energy Release Rate of Plastic Materials. 2007.
(28) Erb, R. M.; Segmehl, J.; Charilaou, M.; Loffler, J. F.; Studart, A. R. *Soft Matter* **2012**, *8*, 7604−7609.
(29) Perrin, F. *J. Phys. Radium* **1934**, *5*, 497−511.
(30) Erb, R. M.; Son, H. S.; Samanta, B.; Rotello, V. M.; Yellen, B. B. *Nature* **2009**, *457*, 999−1002.
(31) Erb, R. M.; Sander, J. S.; Grisch, R.; Studart, A. R. *Nat. Commun.* **2013**, *4*, 1712.
(32) Forsyth, P. A., Jr.; Marčelia, S.; Mitchell, D. J.; Ninham, B. W. *Adv. Colloid Interface Sci.* **1978**, *9*, 37−60.
(33) Mourad, M. C. D.; Petukhov, A. V.; Vroege, G. J.; Lekkerkerker, H. N. W. *Langmuir* **2010**, *26*, 14182−14187.
(34) van der Kooij, F. M.; Lekkerkerker, H. N. W. *J. Phys. Chem. B* **1998**, *102*, 7829−7832.
(35) Onsager, L. *Ann. N.Y. Acad. Sci.* **1949**, *51*, 627−659.
(36) van der Beek, D.; Lekkerkerker, H. N. W. *Langmuir* **2004**, *20*, 8582−8586.
(37) Bonderer, L. J.; Studart, A. R.; Woltersdorf, J.; Pippel, E.; Gauckler, L. J. *J. Mater. Res.* **2009**, *24*, 2741−2754.
(38) Fornes, T. D.; Paul, D. R. *Polymer* **2003**, *44*, 4993−5013.
(39) Halpin, J. C.; Kardos, J. L. *Polym. Eng. Sci.* **1976**, *16*, 344−352.
(40) Shukla, D. K.; Kasisomayajula, S. V.; Parameswaran, V. *Compos. Sci. Technol.* **2008**, *68*, 3055−3063.
(41) Gojny, F. H.; Wichmann, M. H. G.; Kopke, U.; Fiedler, B.; Schulte, K. *Compos. Sci. Technol.* **2004**, *64*, 2363−2371.
(42) Lim, S. H.; Zeng, K. Y.; He, C. B. *Mater. Sci. Eng., A* **2010**, *527*, 5670−5676.
(43) Thostenson, E. T.; Li, C. Y.; Chou, T. W. *Compos. Sci. Technol.* **2005**, *65*, 491−516.
(44) Yu, Z. Q.; You, S. L.; Yang, Z. G.; Baier, H. *Adv. Compos. Mater.* **2011**, *20*, 487−502.
(45) Ashby, M. F. *Materials selection in mechanical design*; Butterworth-Heinemann: Oxford, U.K., 2005; p 603.
(46) *Granta CES* 11.9.9; Granta Design Limited: Cambridge, U.K., 2012.